# Testing conditions for CoMo HDS catalyst in the kinetic region: integrated approach using the math calculations and catalytic experiments

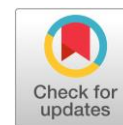Polina P. Mukhacheva [ID], Yuliya V. Vatutina, Ivan A. Mik * [ID],
Ksenia A. Nadeina, Maksim O. Kazakov [ID], Oleg P. Klenov, Oleg V. Klimov [ID],
Aleksandr S. Noskov [ID]

Boreskov Institute of Catalysis SB RAS, Novosibirsk 630090, Russia
* Corresponding author: mikluha.ia@gmail.com

This paper belongs to a Regular Issue.

## Abstract

The main idea of the investigation was to define testing parameters with the lowest influence of internal and external diffusion on catalytic activity in hydrodesulfurization of dibenzothiophene. Traditional experimental methods were used to determine the conditions for the influence of internal and external diffusion. Simultaneous change of a linear feedstock rate and a catalyst loading at constant weight hour space velocity were used to determine the process temperature (240–260 °C) at which the impact of external diffusion is minimal. Catalytic tests, including the variation of the catalyst fraction size, were carried out to define the conditions with the lowest influence of internal diffusion. It was found that when the catalyst with the fraction size of 0.1–0.25 mm was used, the fluctuation of sulfur conversion was the smallest. Besides, to validate experimental results, the calculations were performed with mass balance equations and expressions used for HDS modeling. The resulting data and catalytic experiments demonstrated that the lowest influence of internal and external diffusion is achieved at a temperature process less than 260 °C and a catalyst fraction of 0.1–0.25 mm.

## Key findings

● Testing conditions were consistent with the requirements of the ideal plug flow.
● Conditions with the lowest influence of internal and external diffusion were defined.
● Experimental results are in good agreement with the calculations.

## 1. Introduction

Typical hydrotreating catalysts of diesel fraction are CoMo/Al$_2$O$_3$ catalysts with trilobe or quadrilobe granular shape [1–5]. Nowadays, most of the solutions for improving the hydrotreating catalysts are aimed at tuning active component properties, namely, at the selective formation of the active phase [6–9]. To directly estimate the effect of changes in properties of the active component on catalytic activity, catalytic tests should exclude most of the process interference parameters. When the liquid feedstock contacts with a solid catalyst during hydrotreating, the following processes occur in the reactor: mass transferring of reagents from the liquid volume to the external surface of a catalyst granule (external diffusion), and diffusion of reagents from external catalyst surface into pores and then to active sites that carry out the reaction (internal diffusion). Internal diffusion has the greatest influence on hydrotreating reactions, since these reactions proceed over solid catalysts via contact of feedstock molecules and active sites in pores of a catalyst [10, 11]. It is obvious that the influence of diffusion limitations greatly depends on textural properties of a catalyst, size of granules, reaction conditions and feedstock. So, it is necessary to carry out catalytic tests with low influence of internal and external diffusion on catalytic activity for reliable evaluation of the impact of active component properties on catalytic activity.

There is a good theoretical background [10–13] for describing approaches for testing heterogeneous catalysts in

a flow tube reactor to determine the influence of diffusion limitations on catalyst activity. Catalytic experiments, including proportional changes of a linear feedstock velocity and volume of a catalyst at constant liquid hour space velocity (LHSV), are usually carried out. The influence of external diffusion is considered to be minimal, when the variation of a linear feedstock velocity and catalyst volume does not cause a change in the conversion of the addressed reagent. The influence of diffusion can be indirectly estimated by calculating liquid–solid mass transfer coefficient ($k_s$, cm s$^{-1}$) [11, 14]. When the impact of internal diffusion is the lowest, $k_s$ can be determined by mass balance equations of liquid and solid phases. These equations include effective diffusivity and the mass transfer coefficient. The higher $k_s$, the greater impact of external diffusion [14, 15].

After that, catalytic tests are performed to define the influence of internal diffusion on catalytic activity. The tests include the decrease of catalyst's granular size and activity measurements. When the reduction in granular size does not affect the conversion, the influence of internal diffusion is minimal. [12]. The indirect characteristic used for defining the internal diffusion impact is the catalyst effectiveness factor (η) [11, 14]. When the effectiveness factor is much less than 1, there is an influence of internal diffusion. For example, the effectiveness factor for hydrotreating catalysts with trilobe shape is about 0.3–0.8 for processing model sulfur-containing molecules [14]. When catalysts are tested in hydrotreatment of the real feedstock, the effectiveness factor is usually less than 0.6 [16]. The effectiveness factor should be close to 1 to conduct a correct investigation in the development of hydrotreating catalysts, for example, for the determination of the reaction rate constant, activation energy, etc.

This report presents the testing conditions for CoMo/Al$_2$O$_3$ hydrotreating catalysts in hydrodesulfurization (HDS) of dibenzothiophene (DBT) at the lowest influence of internal and external diffusion. Catalytic experiments were carried out in conditions of ideal plug flow. Therefore, the obtained results can be used by the researchers working in the field of hydrotreating catalysts and can be adapted to their catalysts test conditions. The mass transfer coefficient and the effectiveness factor of the catalyst were defined using the results of catalytic experiments. They were calculated using the mass balance equations and mathematical expressions. These parameters were calculated with known mathematical expressions previously used in HDS modeling [2, 17–27].

## 2. Experimental

### 2.1. Catalyst preparation and characterization

The CoMo/Al$_2$O$_3$ catalyst has been prepared by the following procedure. To prepare impregnating solution, the reagents were sequentially added into the water under stirring in the following order: cobalt hydroxide (Baltic Enterprise, Ltd., Russia, pure), molybdenum oxide (Alfa Aesar, USA,

pure) and phosphoric acid (OJSC "TK Spectr-Khim", Russia, 98%). The reagents were dissolved at 70 °C. After complete dissolution of the reagents, the obtained solution was used for vacuum impregnation of γ-Al$_2$O$_3$ support (produced by OOO «NPK «Synthesis», Russia). Then, the catalyst was dried at 120 °C during 4 h in air flow.

Investigation of the catalyst by nitrogen adsorption-desorption was made according to the procedure described in [28]. The catalyst was calcined at 550 °C before analysis. High-resolution transmission electron microscopy (HRTEM) and X-ray photoelectron spectroscopy (XPS) studies were performed for the catalyst sulfided in H$_2$S flow. The description of the sulfidation procedure is given in [28, 29].

### 2.2. Catalytic experiment

The CoMo/Al$_2$O$_3$ hydrotreating catalyst was used to define the testing conditions with the lowest influence of internal and external diffusion.

**Preparation of the catalyst for testing.** Before testing, the catalyst fraction ($dc_1$ = 0.1–0.25 mm, $dc_2$ = 0.25–0.5 mm and $dc_3$ = 0.5–1.0 mm) was sulfided in a flow-through quartz reactor in H$_2$S flow at atmospheric pressure and a temperature of 220 °C for 2 h and 400 °C for 2 h. The catalyst's fraction was cooled in helium flow.

**Reactor description.** Testing of catalysts was carried out in the fixed-bed flow microreactor in all cases. The reactor had the following characteristics: the diameter ($D_R$) – 8 mm, the bed length ($L_b$) – 40 mm, $D_R/dc_1$ = 80–32, $D_R/dc_2$ = 32–16 and $D_R/dc_3$ = 16–8, $L_b/dc_1$ = 400–160, $L_b/dc_2$ = 160–80 and $L_b/dc_3$ = 80–40. To decrease the temperature gradient and to improve hydrodynamics of the reactor in the catalyst's bed, the sulfide catalyst fraction was uniformly mixed with silicon carbide (the fraction of SiC is 0.1–0.25 mm). Total volume of the mixture of SiC and the catalyst was 4 ml in all cases. It should be noted that conditions of catalytic experiments complied with the ideal plug flow regime: $D_R/dc$>10 and $L_b/dc$>50 [13].

**Model feed description.** The mixture of DBT and undecane was used as the model feedstock. DBT was used as a sulfur-containing compound. DBT content was 14500 ppm (sulfur content is 2500 ppm). Undecane (ρ = 0.74 g/cm$^3$) was used as a solvent.

**Reaction conditions.** The influence of external diffusion was considered to be minimal, when the conversion of the reacting component does not change at variation of a linear feedstock velocity and a catalyst volume and constant LHSV during catalytic tests [12]. In our case, the catalyst fraction loaded to the reactor was less than 1 g, and it was difficult to correctly measure the volume. Therefore, the present catalytic experiments include variation of a linear feedstock velocity ($\vartheta_{feed}$) and catalyst loading ($m_c$) along with the constant weight hour space velocity (WHSV, h$^{-1}$) ($\vartheta_{feed} \cdot \rho_{feed}/m_c$). The experiments were performed using the catalyst fraction of 0.1–0.25 mm. The catalyst loadings $m_c$ = 0.5 g, 0.4 g and 0.3 g, and the linear feedstock velocities $\vartheta_{feed}$ = 54.0 ml h$^{-1}$, 43.2 ml h$^{-1}$ and 32.4 ml h$^{-1}$ were chosen,

while WHSV was 80 h$^{-1}$. The testing conditions were as follows: $p$ = 4 MPa, H$_2$/feedstock ratio = 300 Nm$^3$/m$^3$, $T$ = 240 ºC, 260 ºC and 280 ºC.

The additional experiment was performed to check the influence of internal diffusion limitations. The catalyst fraction ($m_c$ = 0.4 g) with the particle sizes of 0.1–0.25 mm, which was chosen after previous experiments, was used. The following conditions were used: $p$ = 4 MPa, H$_2$/feedstock ratio = 300 Nm$^3$/m$^3$, WHSV = 80 h$^{-1}$, $T$ = 225–280 ºC. The results of the experiment were used to construct a plot of the ln($k$) vs 1000/$T$ dependence. The rate constants of hydrodesulfurization of dibenzothiophene were determined based on the assumption of the pseudo-first order of reaction; equation (1) was used for calculation [3]. This plot allows calculating the activation energy ($E_a$) with the Arrhenius equation (2):

$$k = \frac{-F(DBT)}{W} \cdot \ln\left(1 - \frac{XDBT}{100}\right), \tag{1}$$

where $k$ – rate constant, mol/(g·h), $F$(DBT) – molar flow rate of the feedstock, mol/h, $W$ – catalyst loadings, g, $X_{DBT}$ – conversion of DBT, %.

$$k = k_0 \cdot \exp(-E_a/RT). \tag{2}$$

One of the methods of defining the influence of internal diffusion on catalytic activity consists in carrying out a set of experiments with different size of granules/fraction particles of a catalyst [10, 11, 13]. To determine effect of internal diffusion in HDS of DBT, the experiments were performed. The sizes of the catalyst fraction were $dc_1$ = 0.1–0.25 mm, $dc_2$ = 0.25–0.5 mm and $dc_3$ = 0.5–1.0 mm. The testing conditions were as follows: $p$ = 4 MPa, $T_1$ = 240 ºC, $T_2$ = 260 ºC, ratio H$_2$/feedstock = 300 Nm$^3$/m$^3$, WHSV = 80 h$^{-1}$. The catalyst loadings $m_c$ = 0.5 g was chosen.

In all cases, the time to achieve steady-state of the catalyst was about 12 h. Then, 4 liquid reaction products were sampled at each process temperature. The liquid samples were analyzed using TE Instruments XPLORER for the determination of the residual sulfur content.

Liquid products were analyzed on a PerkinElmer gas chromatograph Clarus 580 to defined residual DBT content. The resulting DBT content was similar for the samples obtained at one temperature regime (the inaccuracy of the method is 5%) that indicates the absence of catalysts deactivation during the catalytic tests.

The conversion of DBT ($X_{DBT}$) was used as a characteristic of catalytic activity. $X_{DBT}$ was calculated according to equation (3):

$$X_{DBT} = \frac{C_{DBT0} - C_{DBT}}{C_{DBT0}} \cdot 100, \tag{3}$$

where $C_{DBT0}$ is the initial DBT content in the model mixture and $C_{DBT}$ is the content of DBT in the hydrotreated product.

## 2.3. The estimation of the HDT reactor parameters

To make the qualitative estimations of the HDT reactor parameters, one must consider the phenomena that can change the reactor performance. Some effects such as axial mass dispersion, catalyst wetting, and wall flow have a macroscopic effect on the mass and heat transfer. Thereby their effect must be analyzed to determine whether they should be considered or not in mass balance equations and mathematical expressions [31].

1. Isothermal operation.

The temperature of the experimental reactor was controlled within ±1 ºC during the collection of the experimental data. For this reason, the reactor was considered isothermal (only the mass balance was taken into account in the calculations.

2. Ideal plug behavior.

It was determined by Chen criterion (2) [31] that the experimental setup does not present plug-flow deviation, since the ratio of catalytic bed length to particle diameter is high enough to avoid back mixing effects. The right-hand side in expression of inequality (4) was 87 , and the left-hand side – 69 (87>69).

$$\frac{L_b}{d_e} > \frac{\sqrt{20}n}{Bo_{a.m}^f} \ln\left(\frac{1}{1 - X/100}\right), \tag{4}$$

where $L_b$ – reactor-bed length, cm, $d_e$ – equivalent size of a catalyst particle, cm, $Bo_{a.m}^f$ – axial mass Bodenstein number for $f$ phase, $n$ – order of reaction.

3. Incomplete wetting.

Complete irrigation of the catalytic bed was ensured by Gierman and Harmsen criterion ($W$, equation (5)), since the wetting number equal to 2·10$^{-1}$ was obtained.

$$W = \frac{\mu_L}{\rho_L d_e^2 g} > 5 \cdot 10^{-6} \tag{5}$$

where $\mu_L$ – viscosity of the liquid phase, mPa s, $\rho_L$ – liquid density at process conditions, lb ft$^{-3}$, $g$ – gravitational constant, cm s$^{-2}$

4. Wall flow effect.

The experimental reactor presents the ratio of the reactor diameter to equivalent diameter of particles equal to 64. It meets the Sie criterion ($\frac{D_R}{d_e}$, equation (6)) [31], decreasing the hydrodynamic problems associated with liquid distribution and wall flow.

$$\frac{D_R}{d_e} > 25. \tag{6}$$

# 3. Description of the mathematical calculations

## 3.1. Characteristics of the catalyst bed and physical properties of the feed

No effect of internal and external diffusion was confirmed through dependences of estimated HDS parameters ($k_s$ and η) for some of the conditions presented in the work. Estimations below were obtained from isothermal small reactor (in this study, $D_R$ = 8 mm) [2, 15, 24, 25, 32, 33].

Mathematical calculations in these works are based on kinetic experimental data, characteristics of the catalyst bed, mass balance equations and other proven chemical engineering expressions. A set of assumptions is assumed in calculating the estimations. The HDS reactor is considered isothermal and steady state operated. Catalyst deactivation was thought to be insignificant. The reaction is assumed to occur only in the porous solid catalyst, which is uniformly wetted by the liquid. Gas and liquid velocities are constant across the reactor. Gas–liquid mass transfer was neglected. The particle diameter of the catalyst was taken as the equivalent diameter of the sphere with the same volume and surface area as those of our catalyst. The diffusion effects for different conditions can be estimated from the values of the sulfur content in the product and the catalyst effectiveness factor. Therefore, below are the equations for simulation of an isothermal HDS reactor that include the conditions for testing and the other ones.

The bed porosities ($\varepsilon_B$) of the catalyst were calculated from the weights of loadings, particles densities and the height of bed in the graduated cylinder (inner diameter 8 mm) [34].

The expressions (7)–(9) can be used to calculate the physical properties of oil and gas at process conditions. The oil density ($\rho_L$) as a function of temperature and pressure can be estimated by the Standing–Katz equation as published in [25, 35]:

$$\rho_L = \rho_0 + \Delta\rho_P - \Delta\rho_T, \tag{7}$$

$$\Delta\rho_P = [0.167 + 16.181 \cdot 10^{-0.0425\rho_0}] \cdot \left[\frac{P}{1000}\right] - 0.01 \cdot$$
$$\cdot [0.299 + 263 \cdot 10^{-0.0603\rho_0}] \cdot \left[\frac{P}{1000}\right]^2, \tag{8}$$

$$\Delta\rho_T = [0.0133 + 152.4 \cdot (\rho_0 + \Delta\rho_P)^{-2.45}] \cdot (T_R - 520) -$$
$$- [8.1 \cdot 10^{-6} - 0.0622 \cdot 10^{-0.764(\rho_0 + \Delta\rho_P)}] \cdot (T_R - 520)^2, \tag{9}$$

where $\rho_0$ – density of oil at 15.6 °C and 101.3 kPa, lb ft$^{-3}$, $\Delta\rho_P$ – pressure dependence of liquid density, lb ft$^{-3}$, $\Delta\rho_T$ – temperature correction of liquid density, lb ft$^{-3}$, $P$ – the pressure, $T_R$ is the temperature, °R.

Glaso's equation, as presented in [18, 19, 35], was used as a generalized mathematical equation for oil viscosity. Equations (10)–(12) are the following:

$$\mu_L = 3.141 \cdot 10^{10}(T - 460)^{-3.444}[\log_{10}(API)]^a, \tag{10}$$

$$a = 10.313[\log_{10}(T - 460)] - 36.447, \tag{11}$$

$$API = \frac{141.5}{d_{15.6}} - 131.5, \tag{12}$$

where $a$ – dimensionless number, API – American Petroleum Institute, $T$ is the temperature (°C), $d_{15.6}$ is the specific gravity of oil at 15.6 °C.

Strictly speaking, equations (7)–(12) for calculating liquid characteristics are valid for petroleum distillates, especially for the ones containing DBT. Considering all

arguments, the given expressions were used for calculating properties of liquid phase. It should be emphasized that these calculations are approximate.

## 3.2. Mass balance equations

HDS of oil fractions can be considered as a bimolecular irreversible reaction between the oil (A) and hydrogen (B) reactants [25, 36]:

$$\nu_A A + \nu_B B \rightarrow \nu_P Prod, \tag{13}$$

where $\nu_A$, $\nu_B$, $\nu_P$ are stoichiometric coefficients of A, B and product, respectively. This simplified equation of the reaction is assumed to be valid for the case presented with DBT.

Mass balance equations for the liquid and solid phases are given below.

Equation for the liquid phase (14):

$$u_L \frac{dC_{sulL}}{dz} + k_s a_t(C_{sulL} - C_{sulS}) = 0 \tag{14}$$

where $k_s$ – the liquid–solid mass transfer coefficient, $u_L$ – the superficial velocity of the liquid in the reactor, cm s$^{-1}$, $a_t$ – surface area of the particles per unit volume of the bed, cm$^{-1}$, $C_{sulL}$ – concentration of sulfur compound in the liquid phase, mol cm$^{-3}$, $C_{sulS}$ – molar liquid phase of sulfur inside the solid, mol cm$^{-3}$, $z$ – coordinate of reactor bed length.

Equation for the solid phase (15):

$$\frac{k_s a_t(C_{sulL} - C_{sulS})}{\nu_A} + (\varepsilon_B - 1)\rho_P \eta k C_{sulS}^n = 0, \tag{15}$$

where $\eta$ is the effectiveness factor, $\varepsilon_B$ – void fraction of the catalyst bed, $k$ – reaction rate coefficient. The value $n = 1$ was used in the presented work. According to the literature data [3], HDS of DBT follows pseudo first reaction order.

HDS kinetic constant ($k$) was estimated only by the original approaches described in [18, 37–39]. The procedure of estimation of the kinetic parameters ($k_0$ and $E_A$) is presented in Supplementary materials. The inhibiting effect of H$_2$S was not taken into account, since its concentration is not high enough. Therefore, the influence of H$_2$S on the HDS reaction rate is not significant.

Since the catalyst particles had a complex shape, the equivalent diameter of the catalyst particle was used to calculate the parameters below. An equivalent size $d_e$ of a catalyst particle can be calculated as (16):

$$d_e = \frac{2V_P}{S_P}, \tag{16}$$

where $V_P$ – volume of the catalyst particle, cm$^3$, $S_P$ – area of the catalyst particle, cm$^2$.

The surface area ($a_t$) of the particles per unit volume of the bed was calculated by equation (17):

$$a_t = \frac{6(1 - \varepsilon_B)}{d_e}, \tag{17}$$

The molecular diffusivity of sulfur in the liquid ($D^L_{sul}$, cm$^2$ s$^{-1}$) is calculated by equation (18) [40]:

$$D_{sul}^L = 8.93 \cdot 10^{-8} \frac{v_L^{0.267} T}{v_{sul}^{0.433} \mu_L}, \qquad (18)$$

where $v_L$ and $v_{sul}$ are molar volume of solute and liquid solvent, respectively, which are estimated with the following equations (19)–(20) [18]:

$$v_i = 0.285(v_{ci}^m)^{1.048} \qquad (19)$$

$$v_c^m = 7.5214 \cdot 10^{-3} \, T_{MeABP}^{0.2896} d_{15.6}^{-0.7666} \qquad (20)$$

where $v_i$ – molar volume, cm³ mol⁻¹, $v_c^m$ – critical specific volume, ft³ mol⁻¹, $v_{ci}^m$ – critical specific volume of the liquid or gas, ft³ mol⁻¹, $T_{MeABP}$ – the mean average boiling point (°R).

Internal diffusion limitations are usually expressed in terms of the catalyst effectiveness factor [41]. The effectiveness factor reported in [42, 43] has to be in the range of 0.0057–1. Because the particle size of the catalyst is small, the effectiveness factor can be estimated as function of Thiele modulus ($\phi$) [16, 44]. For the different catalyst shapes (sphere, cylinder, 2-lobe, 4-lobe, etc.), the effectiveness factor can be calculated using expressions which has been proposed for other authors [42, 45, 46]. The generalized modulus ($\phi_{sul}$) for $n^{th}$-order irreversible reaction is calculated according to (21) [44]. Effective diffusivity of sulfur in the pores of the catalyst (De$_{sul}$, cm² s⁻¹) was determined with the equation (20) [44].

$$\phi_{sul} = \frac{V_p}{S_p}\left[\left(\frac{n+1}{2}\right)\left(\frac{kC_{sulS}^{n-1}\rho_P}{De_{sul}}\right)\right]^{0.5}, \qquad (21)$$

$$De_{sul} = \frac{\theta}{\tau}\left(\frac{1}{1/D_{sul}^L + 1/D_K}\right), \qquad (22)$$

where $\rho_P$ – catalyst particle density, g cm⁻³, $\theta$ – particle porosity, $\tau$ – tortuosity factor, $D_K$ – Knudsen diffusivity, cm² s⁻¹.

The tortuosity factor ($\tau$) generally has a value of 2–7 [41]. Usually, tortuosity factor is assumed to be 4 [16, 25, 41]. Knudsen diffusivity factor ($D_K$) is evaluated as follows (23)–(25) [44, 47]:

$$D_K = 9700 r_g \left(\frac{T}{M_w}\right)^{0.5}, \qquad (23)$$

$$r_g = \frac{2\theta}{S_g \rho_P}, \qquad (24)$$

$$\theta = \rho_P V_g, \qquad (25)$$

where $M_w$ – the molecular weight, $r_g$ – the pore radius, cm, $S_g$ – specific surface area of a catalyst particle, cm² g⁻¹, $V_g$ – pore volume per unit mass of catalyst, cm³ g⁻¹.

In present report, the following equation is employed for determining the values of η (26) [40, 44, 45]:

$$\eta = \frac{3(\phi_{sul}\coth(\phi_{sul}) - 1)}{\phi_{sul}^2}. \qquad (26)$$

Since the shape of the catalyst fractions mostly resembles a spherical shape, we used the effectiveness factor formula for spherical particles in the present calculation.

## 4. Results and Discussion

### 4.1. Description of the catalyst

According to atomic emission spectroscopy data, the CoMo/Al₂O₃ catalyst used for catalytic tests contains 12.4 wt.% Mo, 2.7 wt.% Co and 1.4 wt.% P. The industrial γ-Al₂O₃ (produced by "NPK "Syntez") was used as the support.

Textural characteristics of the support and the catalyst are given in Table 1. The support has the specific surface area of 223 m²/g, the pore volume of 0.5 cm³/g and the average pore diameter of 9 nm. According to the classification described in [48], the shape of nitrogen adsorption-desorption isotherm of the support corresponds to IV(a) type, while the type of hysteresis loop relates to H2(a) (Figure S2). Such characteristics are typical for mesoporous materials with cylindrical shape of pores [48]. The shapes of nitrogen adsorption-desorption isotherm and hysteresis loop of the catalyst are the same as those of the support, confirming that no plugging of significant pore volume by active metals during impregnation occurs. Pore size distribution curves of the catalyst and the support have similar shape, also indicating no plugging of the pores in the catalyst (Figure S2). After supporting of active metals, the specific surface area of the catalyst decreased to 147 m²/g, while pore volume and average pore diameter were similar to those of the support (Table 1).

The catalyst sulfided in H₂S flow was studied by X-ray photoelectron spectroscopy (XPS) method. The resulting Mo3d and Co2p XPS spectra were deconvoluted into several Mo and Co states (Figure 1). It was established that active metals are preferentially presented in the catalysts in the sulfur surrounding (more than 55%). The portion of Mo in the 4+ state (Mo in the MoS₂ composition [49]) is about 72%. The rest of molybdenum is associated to 5+ (13%) and 6+ (13%) which is characteristic of Mo in oxysulfide and oxide states [49]. The fraction of cobalt in the composition of CoMoS phase [50] is about 58%. Cobalt in the catalyst is also present in the composition of individual sulfide – Co$_x$S$_y$ (12%) and Co²⁺ (29%) [49]. The obtained values of the CoMoS phase content in the catalyst are typical for highly active CoMo/Al₂O₃ catalysts [51].

**Table 1** Textural characteristics of γ-Al₂O₃ support and CoMo/Al₂O₃ catalyst.

| Parameter | Specific surface area, m²/g | Pore volume, cm³/g | Average pore diameter, nm | Average slab length, nm | Stacking number |
|---|---|---|---|---|---|
| Al₂O₃ | 223 | 0.5 | 9 | – | – |
| CoMo/Al₂O₃ | 147 | 0.4 | 10 | 3.7 | 2.2 |

The sulfide catalyst was also studied by HRTEM method. The examples of HRTEM images are given in Figure S3. The average slab length and stacking number of active component particles, which were calculated by analysing of several images with more than 500 particles, are 3.7 nm and 2.2, respectively (Table 1). The resulting values are typical of CoMo/Al₂O₃ hydrotreating catalysts [51].

## 4.2. Experimental data on the effect of external and internal diffusion

The data obtained in the HDS experiments to determine the impact of external diffusion are given in Table 2. The conditions of catalytic experiments are described in section 2. These experiments allowed us to determine the temperature, at which the DBT conversion or residual sulfur content remained unchanged while the linear feedstock velocity and the catalyst's loading changed simultaneously at constant WHSV.

The residual sulfur content and DBT conversion are similar at 240 °C and at 260 °C for $\vartheta_{feed}$ = 54.0 and 43.2 ml h$^{-1}$ and $m_c$ = 0.5 g and 0.4 g, respectively (Table 2). DBT conversion is changing in the range of 59–69% at 280 °C. The residual sulfur content at the highest process temperature (280 °C) varies significantly for all catalyst loadings. The greatest difference in residual sulfur content at 280 °C is 252 ppm (Table 2). So, we cannot draw an unequivocal conclusion about the effect of external diffusion at 280 °C from the data obtained. However, we can conclude that the influence of external diffusion is the lowest at 240 °C and at 260 °C ($\vartheta_{feed}$ = 54.0 and 43.2 ml h$^{-1}$).

The next step was to define conditions when the impact of internal diffusion was the smallest. The hydrotreating process was carried out at 240 °C and 260 °C. These temperatures were chosen because of the earlier established minimal influence of external diffusion.

Table 3 shows the data of the HDS experiments to determine the impact of internal diffusion. Experimental conditions are given in section 2. It was found that the influence of internal diffusion is more pronounced for the catalyst fractions 0.25–0.5 mm and 0.5–1.0 mm for both temperatures, since the DBT conversion changed in these cases. Thus, to decrease the contribution of internal diffusion, it is preferable to use the catalyst fraction of 0.1–0.25 mm.

Also, we calculated the value of $E_a$ from the plot of ln($k$) from 1000/$T$. We used this approach for additional

confirmation. For the catalytic experiment, we used the catalyst fraction of 0.1–0.25 mm, according to the results given above (Table 3). The testing temperature varied from 225 to 280 °C. Detailed experimental conditions are given in section 2. The plot is shown in Figure 2. The $E_a$ value was 128.0 kJ/mol. This value is close to that given in [52] for the kinetic region of reaction. So, we can conclude that diffusion influence is minimal in this region. These results partially agree with the results obtained for 240 and 260 °C (Table 2).
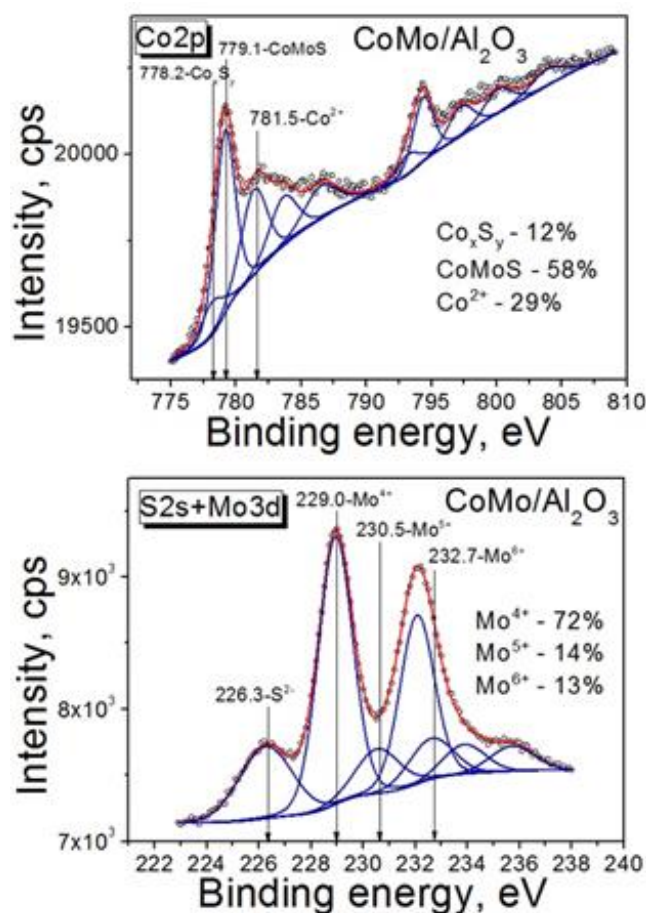


**Figure 1** Mo3d and Co2p XPS spectra.

**Table 3** DBT conversion for catalyst fractions 0.1–0.25 mm, 0.25–0.5 mm and 0.5–1.0 mm at 240 °C and 260 °C.

| Catalyst fraction, mm | 0.1–0.25 | 0.25–0.5 | 0.5–1.0 |
|---|---|---|---|
| Temperature process, °C | $X_{DBT}$, % | | |
| 240 | 11 | 10 | 7 |
| 260 | 37 | 35 | 27 |

**Table 2** Influence of temperature on the residual sulfur content and DBT conversion for the catalyst fraction 0.1–0.25 mm.

| $m_c$, g | $\vartheta_{feed}$, ml h$^{-1}$ | Temperature process, °C | | | | | |
|---|---|---|---|---|---|---|---|
| | | 240 | | 260 | | 280 | |
| | | Residual $S$ content, ppm* | DBT conversion, %** | Residual $S$ content, ppm* | DBT conversion, %** | Residual $S$ content, ppm* | DBT conversion, %** |
| 0.5 | 54.0 | 2224 | 11 | 1745 | 30 | 923 | 63 |
| 0.4 | 43.2 | 2225 | 11 | 1751 | 30 | 773 | 69 |
| 0.3 | 32.4 | 2251 | 10 | 1850 | 26 | 1025 | 59 |

*Inaccuracy of the method for determination of residual sulfur content on TE Instruments XPLORER is 5%.
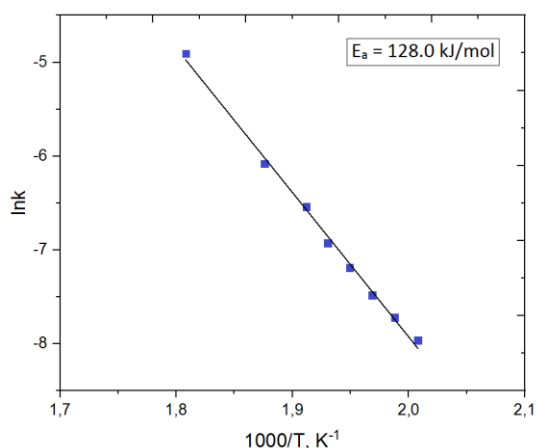** According to PerkinElmer Gas chromatograph Clarus 580 analysis.

**Figure 2** Arrhenius plots of HDS of DBT.

It can be concluded that to minimize the effects of internal and external diffusion it is necessary to test the $CoMo/Al_2O_3$ catalyst in HDS of DBT at a temperature less than 260 °C using the catalyst fraction 0.1–0.25 mm.

### 4.3. Calculated data related to the impact of external and of internal diffusion

Indirect influence of the external diffusion can be estimated by the mass transfer coefficient $k_s$. It should be noted that calculation of this coefficient does not allow us to define the effect of external diffusion. However, effective diffusion in equation (3.16) is used in mass balance equations (3.8) and (3.9). Therefore, it is possible to find the dependence of mass balance coefficient from external diffusion at the negligible effect of internal diffusion.

In the present report, small catalyst fractions (0.1–0.25 and 0.25–0.5 mm) were used. Therefore, the generally accepted equations for calculating $k_s$ cannot be applied [32]. In addition, well-known expressions for $k_s$ cannot be used because some of the parameters, such as phase velocities, do not satisfy the range of acceptable values. Therefore, we used experimental data given in Tables 2 and 3 in the calculations (3.8–3.9).

The data in Table 4 shows that the $k_s$ value for the catalyst fraction 0.1–0.25 mm is lower than that for the catalyst fraction 0.25–0.5 mm at all temperatures. So, the effect of external diffusion will be greater for the larger catalyst (0.25–0.5 mm). The lowest $k_s$ value was obtained at 240 °C. Given the above, the 0.1–0.25 mm catalyst fraction will be less affected by external diffusion at 240 °C.

Then, the effectiveness factor η will be proportional to the impact of internal diffusion because it relates to the ratio of the diffusion reaction rate to the total reaction rate. Therefore, the lower η, the greater the influence of internal diffusion. It allows us to calculate the η value from the equation (3.20). The data in Table 5 demonstrate the effect of the particle size on the effectiveness factor. It should be noted that the value of the effectiveness factor is much closer to 1 for the catalyst fraction 0.1–0.25 mm.

In addition, the performed calculations are used in present work to confirm the behavior of diffusion effects in HDS experiments. The hydrogen flow is in large excess at the reactor inlet in present experimental conditions. Because of the hydrogen-rich atmosphere, the residence time distribution of the gas phase is negligible. Therefore, only the liquid phase hydrodynamic aspects and the mass transport phenomena were analyzed in this report.

The results of the calculations confirm the impact of internal diffusion. The effectiveness factor for the lowest catalyst fraction 0.1–0.25 mm (Table 5) is lower than that for the catalyst fraction 0.25–0.5 mm. Thus, it follows from the observed correlation of the experimental and the calculation data that the influence of internal diffusion is greater, when a larger catalyst fraction was used.

## 5. Limitations

During the improvement and research of hydrotreating catalysts, it is desirable to test catalysts under conditions under which the influence of internal and external diffusion on catalyst activity is minimal. In this case it is possible to establish more reliable correlations between properties of active component particles and catalyst activity. The purpose of this study is to determine such test conditions for hydrotreating catalysts in plug flow regime, under which the influence of internal and external diffusion is minimal.

**Table 5** Effectiveness factor for catalyst fractions 0.1–0.25 mm and 0.25–0.5 mm under different temperature process.

| Catalyst fraction, mm | 0.1–0.25 | 0.25–0.5 |
|---|---|---|
| Temperature process, °C | η | |
| 240 | 0.9423 | 0.8933 |
| 260 | 0.9476 | 0.9025 |
| 280 | 0.9523 | 0.9106 |

**Table 4** Mass transfer coefficient factor for catalyst fractions 0.1–0.25 mm and 0.25–0.5 mm under different temperature process.

| $m_c$, g | $\vartheta_{feed}$, ml h$^{-1}$ | Temperature process, °C | | | | | |
|---|---|---|---|---|---|---|---|
| | | 240 | | 260 | | 280 | |
| | | Catalyst Fraction, mmd | | | | | |
| | | 0.1–0.25 | 0.25–0.5 | 0.1–0.25 | 0.25–0.5 | 0.1–0.25 | 0.25–0.5 |
| | | $k_s \cdot 10^{-2}$, cm s$^{-1}$ | | | | | |
| 0.5 | 54.0 | 0.7329 | 1.4215 | 0.8530 | 1.6743 | 0.9820 | 1.9475 |
| 0.4 | 43.2 | 0.9113 | 1.7690 | 1.0605 | 2.0822 | 1.2553 | 2.4910 |
| 0.3 | 32.4 | 1.1997 | 2.3258 | 1.3853 | 2.7165 | 1.6078 | 3.1839 |

## 6. Conclusions

The conditions for carrying out catalytic tests of the fraction of CoMo/Al$_2$O$_3$ hydrotreating catalyst in the fixed-bed flow microreactor were established. The chosen testing conditions complied with the requirements of ideal plug flow. Simultaneous variation of a linear feedstock velocity (54.0 ml h$^{-1}$, 43.2 ml h$^{-1}$ and 32.4 ml h$^{-1}$) and a catalyst weight (0.5 g, 0.4 g and 0.3 g) at constant WHSV (80 h$^{-1}$) showed that the influence of external diffusion was the lowest at 240–260 °C. The testing of catalysts fractions with the sizes of 0.1–0.25 mm, 0.25–0.5 mm and 0.5–1.0 mm at 240 °C and at 260 °C allowed us to establish that the influence of internal diffusion was minimal for the catalyst fraction of 0.1–0.25 mm. When the catalyst fraction size increased to 0.25–0.5 mm and 0.5–1.0 mm, the effect of the mass transfer of feedstock molecules in catalysts pores to active sites on catalytic activity was observed. The obtained results are in good agreement with the mass transfer coefficient and the effectiveness factor, which were calculated by the mass balance equations and mathematical expressions adapted to the size of the catalyst fraction.

## ● Supplementary materials

This manuscript contains supplementary materials, which are available on the corresponding online page.

## ● Funding

## ● Acknowledgments

None.

## ● Author contributions

Conceptualization: Y.V.V., P.P.M., I.A.M.
Data curation: Y.V.V., P.P.M., K.A.N.
Formal Analysis: P.P.M., I.A.M., O.P.K.
Funding acquisition: O.V.K., A.S.N.
Investigation: P.P.M., Y.V.V., I.A.M., O.P.K.
Methodology: P.P.M., I.A.M., O.P.K.
Project administration: O.V.K., A.S.N.
Supervision: K.A.N., O.V.K., A.S.N.
Validation: M.O.K, O.V.K., A.S.N.
Visualization: P.P.M., Y.V.V., I.A.M.
Writing – original draft: P.P.M., Y.V.V., I.A.M.
Writing – review & editing: P.P.M., Y.V.V., I.A.M., K.A.N.

## ● Conflict of interest

The authors declare no conflict of interest.

## ● Additional information

Author IDs:
Polina P. Mukhacheva, Scopus ID 57226795240;
Yuliya V. Vatutina, Scopus ID 57189731746;
Ivan A. Mik, Scopus ID 55375424900;
Ksenia A. Nadeina, Scopus ID 57218590135;
Maksim O. Kazakov, Scopus ID 23485283300;
Oleg P. Klenov, Scopus ID 6506012360;
Oleg V. Klimov, Scopus ID 7003783535;
Aleksandr S. Noskov, Scopus ID 7005685096.

Website:
Boreskov Institute of Catalysis SB RAS, https://catalysis.ru.

## References

1. Wang TE, Yang F, Song M, Han D. Recent advances in the unsupported catalysts for the hydrodesulfurization of fuel. Fuel Proc Technol.2022:235. doi:10.1016/j.fuproc.2022.107386

2. Ancheyta J. Modeling and simulation of catalytic reactors for petroleum refining. Model Simul Catal Reac Petroleum Refining. 2011. doi:10.1002/9780470933565.fmatter

3. Kaluža L, Gulková D, Šolcová O, Žilková N, Čejka J. Hydrotreating catalysts supported on organized mesoporous alumina: Optimization of Mo deposition and promotional effects of Co and Ni. Appl Catal A Gen. 2008;351(1):93–101. doi:10.1016/j.apcata.2008.09.002

4. Huirache-Acuña R, Navarro Yerga RM, Pawelec B. Hydrodesulfurization on Supported CoMoS$_2$ Catalysts Ex Ammonium Tetrathiomolybdate: Effects of Support Morphology and Al Modification Method. Top Catal. 2022;65:1394–1407. doi:10.1007/s11244-022-01647-w

5. Iqrash Shafiq, Sumeer Shafique, Parveen Akhter, et al. Recent developments in alumina supported hydrodesulfurization catalysts for the production of sulfur-free refinery products: A technical review. Catal Rev. 2020;64:1–86. doi:10.1080/01614940.2020.1780824

6. Klimov OV, Vatutina YV, Nadeina KA. CoMoB/Al$_2$O$_3$ catalysts for hydrotreating of diesel fuel. The effect of the way of the boron addition to a support or an impregnating solution. Catal Today. 2018;305:192–202. doi:10.1016/j.cattod.2017.07.004

7. Zhang C, Zhang Y, Zheng H. Improving both the activity and selectivity of CoMo/δ-Al$_2$O$_3$ by phosphorous modification for the hydrodesulfurization of fluid catalytic cracking naphtha. Energy Fuels. 2022;36(7):3825–3834. doi:10.1021/acs.energyfuels.1c04164

8. Chen Z, Liu Y, Chen J, Zhao Y, et al. Synthesis of alumina-nitrogen-doped carbon support for CoMo catalysts in hydrodesulfurization process. Chin J Chem Engin. 2022;41:392–402. doi:10.1016/j.cjche.2021.09.015

9. Catita L, Quoineaud AA, Moreaud M, Espinat D, Pichon C, Delpoux O. Impact of citric acid on the impregnation of CoMoP/γ-Al$_2$O$_3$ catalysts: time and spatially resolved MRI and Raman imaging study. Top Catal. 2018;61(14):1474–1484. doi:10.1007/s11244-018-1038-7

10. Sun J, Mu C, Li Y, Zhao Y, Wang S, Ma X. The hydrotreatment of n-C16 over Pt/HPMo/SBA-15 and the investigation of diffusion effect using a novel W-P criterion. AIChE J. 2021;67(9):e17330. doi:10.1002/aic.17330

11. Chen A Cheng, Chen SL, Hua D run, et al. Diffusion of heavy oil in well-defined and uniform pore-structure catalyst under hydrodemetallization reaction conditions. Chem Eng J. 2013;231:420–426. doi:10.1016/j.cej.2013.07.035

12. Perego C, Peratello S. Experimental methods in catalytic kinetics. Catal Today. 1999;52(2–3):133–145. doi:10.1016/S0920-5861(99)00071-1

13. Dautzenberg FM. Ten guidelines for catalyst testing. ACS Symposium Ser. 1989:99–119. doi:10.1021/bk-1989-0411.ch011

14. Chen J, Yang H, Ring Z. Study of intra-particle diffusion effect on hydrodesulphurization of dibenzothiophenic compounds. Catal Today. 2005;109(1):93–98. doi:10.1016/j.cattod.2005.08.006

15. PA Ramachandran RC. Three-phase catalytic reactors. Gordon Breach Sci Pub. 1983.

16. Marroquín G, Ancheyta J, Esteban C. A batch reactor study to determine effectiveness factors of commercial HDS catalyst. Catal Today. 2005;104(1):70–75. doi:10.1016/J.CATTOD.2005.03.026

17. Chen J, Mulgundmath V, Wang N. Accounting for vapor-liquid equilibrium in the modeling and simulation of a commercial hydrotreating reactor. Ind Eng Chem Res. 2011;50(3):1571–1579. doi:10.1021/ie101550g

18. Bhaskar M, Valavarasu G, Sairam B, Balaraman KS, Balu K. Three-phase reactor model to simulate the performance of pilot-plant and industrial trickle-bed reactors sustaining hydrotreating reactions. Ind Eng Chem Res. 2004;43(21):6654–6669. doi:10.1021/ie049642b

19. Palos R, Gutiérrez A, Hita I, et al. Kinetic modeling of hydrotreating for enhanced upgrading of light cycle oil. Ind Eng Chem Res. 2019;58(29):13064–13075. doi:10.1021/acs.iecr.9b02095

20. Alvarez-Majmutov A, Chen J. Modeling and simulation of a multibed industrial hydrotreater with vapor-liquid equilibrium. Ind Eng Chem Res. 2014;53(26):10566–10575. doi:10.1021/ie501032j

21. Mijatović IM, Glisic SB, Orlović AM. Modeling a catalytic reactor for hydrotreating of straight-run gas oil blended with fluid catalytic cracking naphtha and light cycle oil: influence of vapor–liquid equilibrium. Ind Eng Chem Res. 2014;53(49):19104–19116. doi:10.1021/ie503188p

22. Jarullah AT, Mujtaba IM, Wood AS. Kinetic model development and simulation of simultaneous hydrodenitrogenation and hydrodemetallization of crude oil in trickle bed reactor. Fuel. 2011;90(6):2165–2181. doi:10.1016/j.fuel.2011.01.025

23. Macías MJ, Ancheyta J. Simulation of an isothermal hydrodesulfurization small reactor with different catalyst particle shapes. Catal Today. 2004;98(1):243–252. doi:10.1016/j.cattod.2004.07.038

24. Mederos FS, Ancheyta J, Elizalde I. Dynamic modeling and simulation of hydrotreating of gas oil obtained from heavy crude oil. Appl Catal A Gen. 2012;425–426:13–27. doi:10.1016/j.apcata.2012.02.034

25. da Rocha Novaes L, de Resende NS, Salim VMM, Secchi AR. Modeling, simulation and kinetic parameter estimation for diesel hydrotreating. Fuel. 2017;209:184–193. doi:10.1016/j.fuel.2017.07.092

26. Korsten H, Hoffmann U. Three-phase reactor model for hydrotreating in pilot trickle-bed reactors. AIChE J. 1996;42(5):1350–1360. doi:10.1002/aic.690420515

27. Shokri S, Zarrinpashne S. A mathematical model for calculation of effectiveness factor in catalyst pellets of hydrotreating process. Pet Coal. 2006;48(1):27–33.

28. Nadeina KA, Danilevich VV, Kazakov MO. Silicon doping effect on the properties of the hydrotreating catalysts of FCC feedstock pretreatment. Appl Catal B Environ. 2021;280:119415. doi:10.1016/j.apcatb.2020.119415

29. Vatutina YV, Kazakov MO, Nadeina KA. Is it possible to reactivate hydrotreating catalyst poisoned by silicon? Catal Today. 2021;378:43–56. doi:10.1016/j.cattod.2021.03.005

30. Fogler SH. Essentials of chemical reaction engineering: essenti chemica reactio engi. Pearson Education; 2010.

31. Mederos FS, Ancheyta J, Chen J. Review on criteria to ensure ideal behaviors in trickle-bed reactors. Appl Catal A Gen. 2009;355(1):1–19. doi:10.1016/j.apcata.2008.11.018

32. Rodríguez MA, Ancheyta J. Modeling of hydrodesulfurization (HDS), hydrodenitrogenation (HDN), and the hydrogenation of aromatics (HDA) in a vacuum gas oil hydrotreater. Energy Fuels. 2004;18(3):789–794. doi:10.1021/ef030172s

33. Felder R. Catalytic reactor design, by M. Orhan tarhan. McGraw-Hill, 1983. B: Aiche J. 1984:372.

34. Mik IA, Klenov OP, Kazakov MO, Nadeina KA, Klimov O V, Noskov AS. Optimization of grading guard systems for trapping of particulates to prevent pressure drop buildup in gas oil hydrotreater. Fuel. 2021;285:119149. doi:10.1016/j.fuel.2020.119149

35. Ahmed T. Hydrocarbon Phase Behaviour . Gulf, Houston, TX. 1989:226.

36. Biardi G, Baldi G. Three-phase catalytic reactors. Catal Today. 1999;52(2):223–234. doi:10.1016/S0920-5861(99)00077-2

37. Ancheyta J, Angeles MJ, Macías MJ, Marroquín G, Morales R. Changes in apparent reaction order and activation energy in the hydrodesulfurization of real feedstocks. Energy Fuels. 2002;16(1):189–193. doi:10.1021/ef0101917

38. Ancheyta-Juárez J, Aguilar-Rodríguez E, Salazar-Sotelo D, Betancourt-Rivera G, Leiva-Nuncio M. Hydrotreating of straight run gas oil-light cycle oil blends. Appl Catal A Gen. 1999;180(1–2):195–205. doi:10.1016/S0926-860X(98)00351-2

39. Macías Hernández MJ, Morales RD, Ramírez-Lopez A. Simulation of the effectiveness factor for a tri-lobular catalyst on the hydrodesulfurization of diesel. 2009;7(1). doi:10.2202/1542-6580.1806

40. Duduković MP, Larachi F, Mills PL. Multiphase catalytic reactors: a perspective on current knowledge and future trends. Catal Rev. 2002;44(1):123–246. doi:10.1081/CR-120001460

41. Satterfield CN. Trickle-bed reactors. AlChE J. 1975;21(2):209–228.

42. Li C, Chen YW, Tsai MC. Highly restrictive diffusion under hydrotreating reactions of heavy residue oils. Ind Eng Chem Res. 1995;34(3):898–905. doi:10.1021/ie00042a024

43. Scamangas A, Papayannakos N, Marangozis J. Catalytic hydrodesulfurization of a petroleum residue. Chem Eng Sci. 1982;37(12):1810–1812.

44. G. F. Froment, K.B. Bischoff J de W. Chemical reactor analysis and design. 1990.

45. Chang J, Liu J, Li D. Kinetics of resid hydrotreating reactions. Catal Today. 1998;43(3–4):233–239. doi:10.1016/S0920-5861(98)00152-7

46. Aris R. The Mathematical Theory of Diffusion and Reaction in Permeable Catalysts: The theory of the steady state. Oxford Uni.; 1975.

47. Carberry JJ. Chemical and Catalytic Reaction Engineering. Courier Corporation; 2001.

48. Thommes M, Kaneko K, Neimark A V., et al. Physisorption of gases, with special reference to the evaluation of surface area and pore size distribution (IUPAC Technical Report). Pure Appl Chem. 2015;87(9–10):1051–1069. doi:10.1515/pac-2014-1117

49. Wang HW, Skeldon P, Thompson GE. XPS studies of MoS2 formation from ammonium tetrathiomolybdate solutions. Surf Coatings Technol. 1997;91:200–207. doi:10.1016/S0257-8972(96)03186-6

50. Gandubert AD, Legens C, Guillaume D, Payen E. X-ray photoelectron spectroscopy surface quantification of sulfided CoMoP catalysts – relation between activity and promoted sites – Part I: influence of the Co/Mo Ratio. Surf Interface Anal. 2006;38:206–209. doi:10.1002/sia.2249

51. Vatutina Y V, Klimov O V, Stolyarova EA, et al. Influence of the phosphorus addition ways on properties of CoMo-catalysts of hydrotreating. Catal Today. 2019;329:13–23. doi:10.1016/j.cattod.2019.01.005

52. Pecoraro T.A., Chianelli R.R. Hydrodesulfurization catalysis by transition metal sulfides. J Catal. 1981;67:430. doi:10.1016/0021-9517(81)90303-1